JOURNAL OF MATERIALS SCIENCE 30 (1995) 5449–5456

Thermodynamic stability of silicon oxycarbide $Si_5C_6O_2$ (Nicalon)

M. NAGAMORI, J.-A. BOIVIN, A. CLAVEAU
Centre de Recherches Minérales, Quebec Government, Ste-Foy, Quebec G1P 3W8, Canada

The standard entropy and heat of formation of amorphous silicon oxycarbide, $Si_5C_6O_2$, have been assessed to be 161.1 $J\,K^{-1}\,mol^{-1}$ and $-1282.3\,kJ\,mol^{-1}$, respectively, based in part on the literature data of the mass-spectrometric vapour pressure of SiO(g) over a Nicalon fibre. Using the so-obtained standard Gibbs energy of $Si_5C_6O_2$, new phase relations (predominance diagrams) of the Si–C–O system have been computed and graphically shown for the temperature range 300–2400 K, including such condensed phases as C, Si, SiC, Si_2O, SiO, Si_2O_3, SiO_2 and $Si_5C_6O_2$. The thermal behaviour of Nicalon fibres can be quantified thermodynamically by use of the predominance diagrams.

1. Introduction

The ceramic filament synthesized from a melt-spun precursor of polycarbosilanes was first thought to be a SiC fibre, as reported by Yajima *et al.* [1] in 1975. It took several years before oxygen was recognized as an essential component of this ceramic glass [2]. Today, Yajima's ceramic fibre is known to be an amorphous phase of silicon oxycarbide, and is available commercially [3] under trademarks such as Nicalon (Nippon Carbon, Tokyo).

In order to characterize the thermal behaviour of silicon oxycarbide, thermodynamic properties such as the heat and Gibbs energy of formation, standard entropy, and heat capacity have to be known corresponding to a given chemical formula. None of these values is found in the literature. The present study was undertaken to calculate these missing data with the use of the latest data on the Si–O [4] and Si–C systems [5], as well as the mass-spectrometric vapour pressure of SiO gas over Nicalon, as reported by Johnson *et al.* [6, 7]. The thermodynamic data were then used to define the thermal stability of silicon oxycarbide under diverse conditions.

2. Chemical composition of Nicalon fibres

The X-ray diffraction and other physical investigations have established Nicalon as an amorphous solid solution of the Si–C–O system [2, 8, 9]. Thus, Nicalon can have varying chemical compositions and still remain homogeneous. It is convenient to express the composition of this oxycarbide glass by the formula $SiC_\alpha O_\beta$, where the subscripts α and β refer to the respective atomic ratios C/Si and O/Si in oxycarbide. The chemical compositions reported by different researchers [10–18] are plotted in Fig. 1 using the indices α and β.

Some of the reported compositions are not of homogeneous silicon oxycarbide, but resulted from the oxidation or decomposition of Nicalon (NIC) at higher temperatures. For example, it appears that the point 7 by Ishikawa *et al.* [3] represents a heterogeneous mixture of NIC + SiO_2, whereas the points P by Porte and Sartre [16] consist of NIC + C(graphite). By analysing these compositional observations in terms of the Gibbs phase rule, the solubility limits about Nicalon can be estimated as shown in Figs 1 and 2. The average Nicalon composition may be expressed by the stoichiometric formula $Si_5C_6O_2$ or $SiC_{1.2}O_{0.4}$, as marked in Fig. 2. Also shown for comparison in Figs 1 and 2 are the two oxycarbide compositions observed by Belot *et al.* [11] and Colson's old formula $Si_2C_3O_2$ [19]; their preparation methods are different from that of Nicalon fibres.

3. Vapour pressure of SiO(g) over Nicalon

Johnson *et al.* [6, 7] reported two sets of data for the mass-spectrometric vapour pressure (p, atm; 1 atm = 101.3 kPa) of SiO(g) over Nicalon $SiC_{1.25}O_{0.3}$ at 1273–1673 K (kelvin). Their later data [7] were based on an improved experimental method, which produced p_{SiO} values that were about ten times higher than in their previous publication [6]. Both sets of data are reproduced in Fig. 3, where log refers to common logarithm, as throughout this article, and $\log p_{SiO}\,(atm) \equiv Z$.

They mentioned that their experimental SiO vapour pressures tended to be lower due to kinetic factors such as slow diffusions in the glass phase or the formation of a silica crust on the exterior surfaces of finely ground fibres. In the present work, therefore, their highest p_{SiO} data points [7] only were taken into consideration, thereby ignoring all of their earlier measurements [6].

To calculate the heat of formation and a complete set of thermodynamic data from these p_{SiO} values, it takes several assumptions and approximations as well

0022–2461

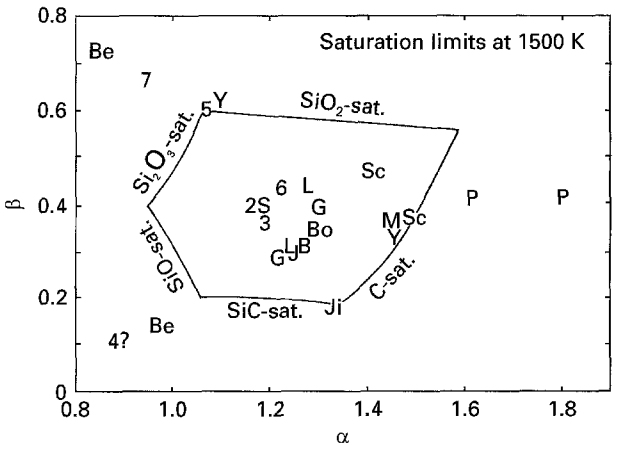

Figure 1 Composition range expressed by the indices α and β of single- and multi-phased Nicalon $SiC_\alpha O_\beta$. Sources: points 2–7 [3]; B [10]; Be [11]; Bo [8]; G [12]; J [6,7]; Ji [13]; L [14]; M [15]; P [16]; S [17]; Sc [18]; Y [2].

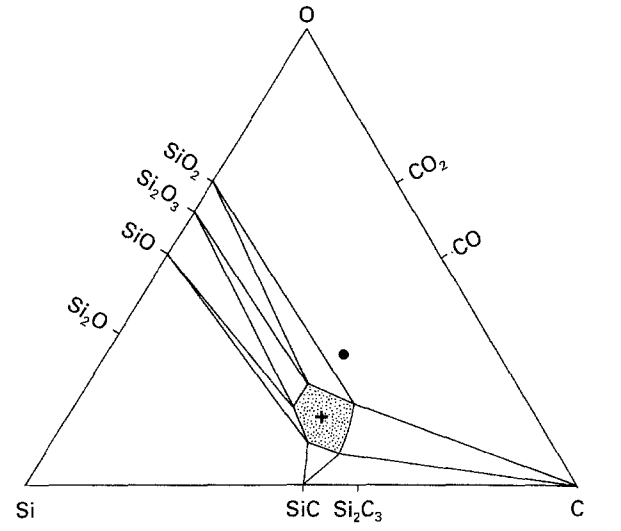

Figure 2 Homogeneous solid solution range (stippled zone) of silicon oxycarbide (Nicalon), limited by the saturation with SiO_2, Si_2O_3, SiO, SiC or C at 1500 K. (+) $Si_5C_6O_2$, (●) Colson's formula $Si_2C_3O_2$ [19].

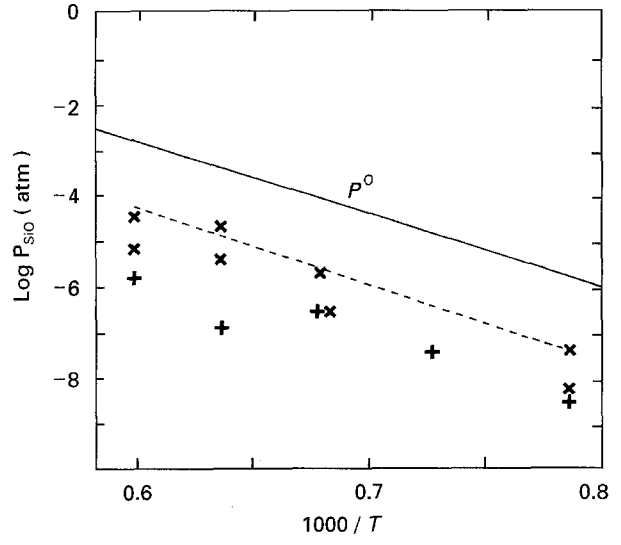

Figure 3 Partial pressure of SiO(g) observed over Nicalon $SiC_{1.25}O_{0.3}$; (+) [6], (×) [7]. P^0 refers to the SiO(g) vapour pressure over pure SiO(am). 1 atm = 101.3 kPa.

as the standard entropy, heat, and Gibbs energy of formation of various substances of the Si–C–O system. The literature data [4, 5, 20, 21] needed for the present thermodynamic calculations are summarized in Tables I and II.

4. Thermodynamic model

4.1. Equilibrium mass balance for $SiC_\alpha O_\beta$ decomposition

The thermal decomposition of silicon oxycarbide, $SiC_\alpha O_\beta$, yielding solid SiC together with CO and SiO gases, can be expressed by the following mass balance

$$SiC_\alpha O_\beta = \frac{1}{2}(1 + \alpha - \beta)\,SiC + \frac{1}{2}(-1 + \alpha + \beta)\,CO + \frac{1}{2}(1 - \alpha + \beta)\,SiO(g) \quad (1)$$

where the product SiC may remain dissolved in silicon oxycarbide as solid solution without forming a separate phase, and therefore its Raoultian activity, a, is smaller than unity, or $a_{SiC} < 1$. The mole ratio, r, of two gaseous products, CO(g) and SiO(g), in Reaction 1 (R1) is dictated solely by the instant chemical composition of silicon oxycarbide, or by α and β, and it may be expressed by

$$r \equiv p_{CO}/p_{SiO} = (-1 + \alpha + \beta)/(1 - \alpha + \beta) \quad (2)$$

As long as some undecomposed $SiC_\alpha O_\beta$ exists in the system, such as at the outset of a decomposition experiment [6, 7], the equilibrium constant K_{R1} of Reaction 1 (R1) can be calculated by

$$K_{R1} = r^{(\alpha+\beta-1)/2}\,(a_{SiC})^{(\alpha-\beta+1)/2}\,(p_{SiO})^{\beta} \quad (3)$$

The Gibbs energy of Reaction 1 at a temperature T, ΔG^0_{R1} J mol^{-1}, can be calculated by substituting K_{R1} and T in the relation

$$\Delta G^0_{R1} = -4.573j\,T \log K_{R1} \quad (4)$$

where $j \equiv 4.185$.

When the values of $\alpha = 1.25$ and $\beta = 0.3$ are inserted into Equation 2, corresponding to the Nicalon used by Johnson *et al.* [6, 7], a value of $r = 11$ results. On the other hand, their experimental ratios r were mostly smaller than 2. This discrepancy was interpreted as indicating that the partial pressures of non-condensable CO(g) were more difficult to measure than those of condensable SiO(g) by their mass-spectrometric technique. Thus, only the observed p_{SiO} was used in the present calculations.

4.2. Heat capacity of $SiC_\alpha O_\beta$

The heat capacities (C°_p J K^{-1} mol^{-1}) of amorphous Si_2C_3 and SiC_2 were calculated by applying a quadratic interpolating function to the known values of silicon, SiC and graphite [5, 20, 21]. The heat capacities of amorphous Si_2O_3, SiO and Si_2O were calculated from the literature data of SiO_2(am) and Si(s) by means of Neumann–Kopp's additivity rule [4, 20]. These data are summarized in Table I. The heat capacities of silicon oxycarbides $SiC_{1.25}O_{0.3}$ and

TABLE I Standard entropy, heat of formation and heat capacity for the Si–C–O system

Species	S°_{298} (J K^{-1} mol^{-1})	ΔH°_{298} (kJ mol^{-1})	C°_p (J K^{-1} mol^{-1})	Reference
C (gr)	$1.361j$[a]	0	$4.10j + 1.02j \times 10^{-3} T - 2.10j \times 10^5 T^{-2}$	[20, 21]
CO (g)	$47.3j$	$-26.4j$	$6.79j + 0.98j \times 10^{-3} T - 0.11j \times 10^5 T^{-2}$	[20, 21]
O_2 (g)	$49.0j$	0	$7.16j + 1.0j \times 10^{-3} T - 0.40j \times 10^5 T^{-2}$	[20, 21]
Si (s)	$4.50j$	0	$5.46j + 0.92j \times 10^{-3} T - 0.85j \times 10^5 T^{-2}$	[20, 21]
SiC (s)	$3.95j$	$-17.5j$	$8.93j + 3.0j \times 10^{-3} T - 3.07j \times 10^5 T^{-2}$	[20, 21]
Si_2C_3 (am)	$8.575j$	$-149.77j$	$21.60j + 7.60j \times 10^{-3} T - 8.25j \times 10^5 T^{-2}$	[5]
SiC_2 (am)	$4.80j$	$-75.59j$	$12.72j + 4.47j \times 10^{-3} T - 5.16j \times 10^5 T^{-2}$	[5]
SiO (am)	$14.72j$	$-101.81j$	$9.94j + 1.84j \times 10^{-3} T - 1.73j \times 10^5 T^{-2}$	[4]
SiO (g)	$50.55j$	$-23.2j$	$7.22j + 1.11j \times 10^{-3} T$	[21], this work
Si_2O_3 (am)	$25.25j$	$-321.46j$	$23.32j + 5.52j \times 10^{-3} T - 5.18j \times 10^5 T^{-2}$	[4]
$SiC_{1.25}O_{0.3}$	$6.8j \pm 0.8j$	$-51.1j \pm 1.2j$	$11.13j + 3.70j \times 10^{-3} T - 3.97j \times 10^5 T^{-2}$	This work
$SiC_{1.20}O_{0.4}$	$7.7j \pm 0.9j$	$-61.3j \pm 1.5j$	$11.46j + 3.60j \times 10^{-3} T - 3.88j \times 10^5 T^{-2}$	This work

[a] $j = 4.185$.

TABLE II Standard Gibbs energy of formation for the Si–C–O system

No.	Reaction	Standard Gibbs energy (J mol^{-1})
1	$Si(s) + O_2 = SiO_2(am)$	$\Delta G^\circ_1 = -216\,817j^a + 56.07j\,T - 4.37jT \log T$
1	$Si(l) + O_2 = SiO_2(am)$	$\Delta G^\circ_1 = -231\,281j + 79.37j\,T - 8.93jT \log T$
2	$2Si(s) + 1.5\,O_2 = Si_2O_3(am)$	$\Delta G^\circ_2 = -322\,879j + 80.23j\,T - 7.38jT \log T$
2	$2Si(l) + 1.5\,O_2 = Si_2O_3(am)$	$\Delta G^\circ_2 = -337\,805j + 105.53j\,T - 12.47jT \log T$
3	$Si(s) + 0.5\,O_2 = SiO(am)$	$\Delta G^\circ_3 = -101\,592j + 22.43j\,T - 2.69jT \log T$
3	$Si(l) + 0.5\,O_2 = SiO(am)$	$\Delta G^\circ_3 = -108\,320j + 17.74j\,T$
4	$2Si(s) + 0.5\,O_2 = Si_2O(am)$	$\Delta G^\circ_4 = -819\,56j + 11.52j\,T - 3.45jT \log T$
4	$2Si(l) + 0.5\,O_2 = Si_2O(am)$	$\Delta G^\circ_4 = -898\,57j + 5.06j\,T$
5	$SiO(am) = SiO(g)$	$\Delta G^\circ_5 = 803\,73j + 74.177j\,T + 12.04jT \log T$
6	$Si(s) = Si(l)$	$\Delta G^\circ_6 = 133\,69j - 13.83j\,T + 1.83jT \log T$
7a	$Si(s) + C(gr) = SiC(s)$	$\Delta G^\circ_7 = -175\,40j + 2.058j\,T$
7b	$Si(s) + C(gr) = SiC(s)$	$\Delta G^\circ_7 = -171\,60j + 1.721j\,T$
7	$Si(l) + C(gr) = SiC(s)$	$\Delta G^\circ_7 = -304\,39j + 9.602j\,T$
8	$C(gr) + 0.5\,O_2 = CO(g)$	$\Delta G^\circ_8 = -273\,40j - 20.50j\,T$
9	$5Si(s) + 6C(gr) + O_2 = Si_5C_6O_2(am)$	$\Delta G^\circ_9 = -308\,904j + 71.222j\,T - 9.194jT \log T$
9	$5Si(l) + 6C(gr) + O_2 = Si_5C_6O_2(am)$	$\Delta G^\circ_9 = -375\,749j + 140.372j\,T - 18.344jT \log T$

[a] $j = 4.185$.

Note: The temperature range of the reactions involving Si (s) is between 298 and 1685 K, while that for the reactions involving Si (l) is between 1685 and 2500 K. The Gibbs energy of Reaction 7a is valid between 298 and 1130 K, and that of Reaction 7b is valid between 1130 and 1685 K. The heats of transformation from the amorphous solid to liquid state of silicon oxides have been neglected. The data for Reaction 9 are from the present work, while the others are quoted from the literature [4, 5, 20, 21].

$SiC_{1.2}O_{0.4}$ may be assessed also by applying Neumann–Kopp's rule to the following pseudobinary systems

$$SiC_{1.25}O_{0.3} \approx 0.1\ Si_2O_3 + 2.05\ Si_{0.39}C_{0.61} \quad (5)$$

$$SiC_{1.25}O_{0.3} \approx 0.3\ SiO\ (am) + 1.95\ Si_{0.36}C_{0.64} \quad (6)$$

$$SiC_{1.2}O_{0.4} \approx 0.133\ Si_2O_3 + 1.933\ Si_{0.38}C_{0.62} \quad (7)$$

$$SiC_{1.2}O_{0.4} = 0.4\ SiO\ (am) + 0.6\ SiC_2 \quad (8)$$

The average values of the so-estimated heat capacities are listed in Table I.

4.3. Standard entropy of $SiC_\alpha O_\beta$

The standard entropy values (S°_{298} J K^{-1} mol^{-1}) for the Si–C and Si–O system compounds [4, 5] are listed in Table I. The approximate entropy values of silicon oxycarbides $SiC_{1.25}O_{0.3}$ and $SiC_{1.2}O_{0.4}$ may be assessed by interpolation of the Si–C and Si–O system values along the pseudobinaries given by Equations 5–8. The standard entropy values thus estimated at 298 K are 6.0 j, 7.6 j, 6.6 j and 8.77 j J K^{-1} mol^{-1} corresponding to Equations 5–8, respectively. The average values adopted for $SiC_{1.25}O_{0.3}$ and $SiC_{1.2}O_{0.4}$ are listed in Table I.

4.4. Activity of SiC in $SiC_\alpha O_\beta$

The Raoultian activity of SiC, a_{SiC}, in $SiC_{1.25}O_{0.3}$ is appreciably smaller than unity because this composition is distanced from the SiC saturation line, as shown in Fig. 1. One may assume a value of $a_{SiC} \approx 0.7$ as starting crude estimate. To improve this approximate value, a series of regression analyses has to be carried out. Starting with calculation of the Gibbs energy by Equation 4, the SiC activities have to be computed eventually for all the uninvariant points such as NIC + SiO_2 + C, NIC + SiO_2 + Si_2O_3, and NIC + Si_2O_3 + SiO at a given temperature. This is

then followed by the construction of a mathematical model to express a_{SiC} as a function of overall $SiC_\alpha O_\beta$ composition. The procedure is repeated until the final model value coincides with the initial crude estimate of a_{SiC}. The following expression was found fit to describe the SiC activity in homogeneous $SiC_\alpha O_\beta$

$$a_{SiC} = (3.86 - 0.836\alpha - 4.288\beta)\,\alpha/(1 + \alpha + \beta) \quad (9)$$

where the numerical coefficients were optimized at 1500 K. For the composition of $SiC_{1.25}O_{0.3}$, Equation 9 gives $a_{SiC} = 0.749$.

5. Results

5.1. Heat of formation of $SiC_{1.25}O_{0.3}$

The value of ΔG°_{R1} is calculated by substituting a selected p_{SiO} in Equations 3 and 4. By combining the so-obtained data of ΔG°_{R1} with the Gibbs energies of SiC, SiO(g) and CO (listed in Table II), the standard Gibbs energy of $SiC_{1.25}O_{0.3}$, ΔG°_{R10} J mol^{-1}, can be calculated corresponding to the following reaction 10 (R10)

$$Si(s) + 1.25\,C(gr) + 0.15\,O_2 = SiC_{1.25}O_{0.3}(am) \quad (10)$$

The standard heat of formation of $SiC_{1.25}O_{0.3}$(am), ΔH°_{298}(R10) J mol^{-1}, can then be obtained by virtue of the Gibbs-Helmholtz equation

$$\Delta H^\circ_{298}(R10) = \Delta G^\circ_{R10} + T\Delta S^\circ_{298} - Q_x \quad (11)$$

where the term Q_x is a function of heat capacity and can be computed by

$$Q_x = \int_{298}^{T} \Delta C^\circ_p\,dT - T\int_{298}^{T} (\Delta C^\circ_p/T)\,dT \quad (12)$$

The terms ΔS°_{298} in Equation 11 and ΔC°_p in Equation 12 are the differences in entropy and heat capacity (Table I), respectively, between the products and reactants in Reaction 10. The actual computation of Equation 11 by substitution of the highest values of log p_{SiO} (Fig. 3) yields the following heat of formation

$$\Delta H^\circ_{298}(R10) = -51.1j \pm 1.2j \text{ kJ mol}^{-1} \quad (13)$$

5.2. Heat of formation of $SiC_{1.2}O_{0.4}$

In order to estimate the standard heat of formation of one formula mole of $SiC_\alpha O_\beta$ in the vicinity of $SiC_{1.25}O_{0.3}$, the following ternary regularity model [22] was devised for a solid solution consisting of $6.022\,(1 + \alpha + \beta) \times 10^{23}$ atoms: namely

$$\Delta H^\circ_{298}(\alpha, \beta) = (K_1\alpha + K_2\beta + K_3\alpha\beta)/(1 + \alpha + \beta) \quad (14)$$

where a value of $K_1 \equiv -28.95j$ kJ mol^{-1} was obtained by referring to an approximate composition of Si_2C_3 in the Si–C binary system [5], and a value of $K_2 \equiv -267.88j$ kJ mol^{-1} was found relative to an average composition between SiO and Si_2O_3 in the Si–O binary [4], while the coefficient K_3 was determined as $K_3 = -36.32j$ kJ mol^{-1} based on the above-obtained ternary heat of formation of $SiC_{1.25}O_{0.3}$. With the use of Equation 14, the standard heat of formation of $SiC_{1.2}O_{0.4}$(am) by Reaction 15 (R15) can be calculated as

$$Si(s) + 1.2\,C(gr) + 0.2\,O_2 = SiC_{1.2}O_{0.4}(am) \quad (15)$$

$$\Delta H^\circ_{298}(R15) = -61.3j \pm 1.5j \text{ kJ mol}^{-1} \quad (16)$$

5.3. Standard Gibbs energy of $Si_5C_6O_2$

Now that the heat of formation is established for $SiC_{1.2}O_{0.4}$ by Equation 16, its combination with heat capacity (Section 4.2) and entropy (Section 4.3) permits calculation of the standard Gibbs energy for any temperature. A regression analysis was applied to the Gibbs energy values thus calculated for 300–1685 K in order to obtain the conventional three-term expression for $Si_5C_6O_2$. The calculated result is given in Table II.

5.4. Internal verification of methodology

As mentioned earlier, the CO/SiO gas ratio observed by Johnson *et al.* [6, 7] did not agree with their initial Nicalon composition (which was supplied only by the manufacturer). Had their Nicalon had an approximate composition of $SiC_{1.2}O_{0.4}$, their r values would have been about 3, which is closer to the observed ratios of $r < 2$. If one assumes that their Nicalon actually was $SiC_{1.2}O_{0.4}$, instead of $SiC_{1.25}O_{0.3}$ as reported, the present thermodynamic procedure then yields a value of

$$\Delta H^\circ_{298}(R15) = -63.6j \pm 3.4j \text{ kJ mol}^{-1} \quad (17)$$

corresponding to Reaction 15 or $SiC_{1.2}O_{0.4}$. The value of Equation 16 is found within the experimental scatter of Equation 17. This indicates that the possible error caused by the currently adopted theoretical value of $r = 11$, rather than the experimental values of $r < 2$, would be smaller than $2.5j$ kJ mol^{-1} on the final outcome of the standard heat of formation of $SiC_{1.2}O_{0.4}$.

Independently, Shimoo and Okamura [23] measured the CO/SiO gas ratio during the thermal decomposition of Nicalon $SiC_{1.2}O_{0.4}$ at 1673 K by means of thermogravimetry coupled with chemical analysis. Their experimental CO/SiO ratios were in fact very close to the theoretical value r formulated by Equation 2. It should be noted that Equation 2 is not valid when SiO_2(am), Si_2O_3(am), SiO(am) or C(gr) is comprised in the decomposition products.

6. Discussion

6.1. Predominance diagram of the Si–C–O system

According to the Gibbs phase rule, the stability conditions of a condensed phase in the Si–C–O system can be defined by two concentration variables at a given temperature. It is most practical [24, 25] to specify these two variables in terms of the partial pressure of CO gas, p_{CO}, and the Raoultian activity of carbon, a_C, or X ($\equiv \log p_{CO}$) and Y ($\equiv \log a_C$). A rather abstract concept of carbon activity may be expressed numer-

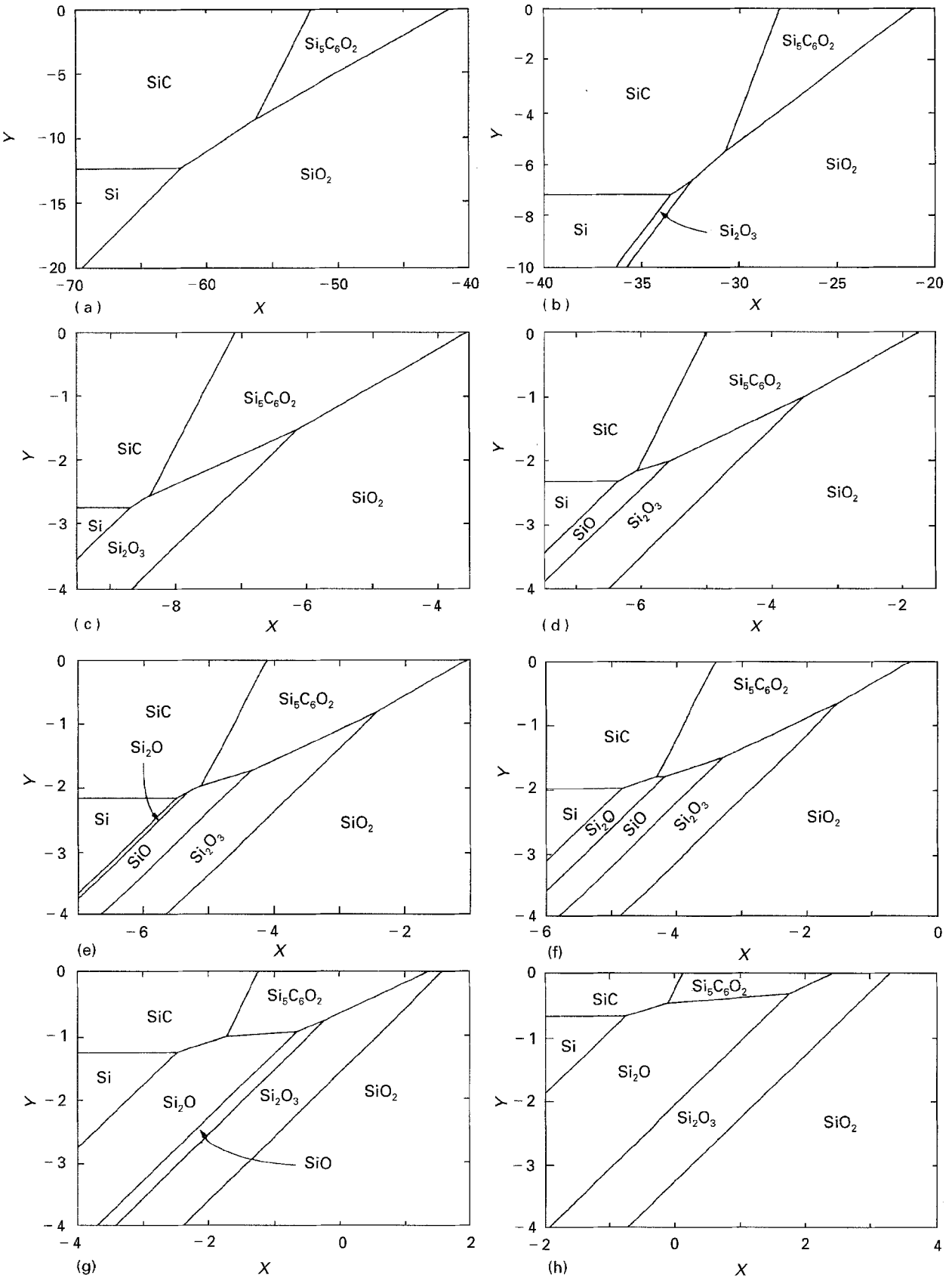

Figure 4 Predominance diagrams of the Si–C–O system at 300–2400 K, as functions of the partial pressure of CO gas (p_{CO}, atm) and the Raoultian activity of graphite, a_C; $X \equiv \log p_{CO}$, $Y \equiv \log a_C$. (a) 300 K, (b) 500 K, (c) 1200 K, (d) 1400 K, (e) 1500 K, (f) 1600 K, (g) 2000 K, (h) 2400 K.

ically, for example, by the partial pressures of CO and CO_2 in the gas phase [20] coexisting with a condensed phase: i.e.

$$a_C = (p_{CO}^2/p_{CO_2}) \exp(20\,045\ T^{-1} - 20.58) \quad (18)$$

The thermodynamic stability of all the condensed phases in the Si–C–O system can be shown graphically by preparing the classical Kelloggian predominance diagram with X and Y as coordinates [24, 25].

TABLE III Equilibrium partial pressure of SiO gas, log p_{SiO} ($\equiv Z$), over various condensed phases in the Si–C–O system as functions of CO partial pressure, log p_{CO} ($\equiv X$), and carbon activity, log a_C ($\equiv Y$)

Phase	Partial pressure of SiO (g); $\kappa = -0.218\,67/T$ [a]
Si	$Z = \kappa(\Delta G_3^\circ + \Delta G_5^\circ - \Delta G_8^\circ) + X - Y$
SiC	$Z = \kappa(\Delta G_3^\circ + \Delta G_5^\circ - \Delta G_7^\circ - \Delta G_8^\circ) + X - 2Y$
$Si_5C_6O_2$	$Z = 0.2\kappa(5\Delta G_3^\circ + 5\Delta G_5^\circ - 3\Delta G_8^\circ - \Delta G_9^\circ) + 0.6X - 1.8Y$
Si_2O	$Z = 0.5\kappa(2\Delta G_3^\circ + 2\Delta G_5^\circ - \Delta G_4^\circ - \Delta G_8^\circ) + 0.5X - 0.5Y$
SiO	$Z = \kappa\,\Delta G_5^\circ$
Si_2O_3	$Z = 0.5\kappa(2\Delta G_3^\circ + 2\Delta G_5^\circ + \Delta G_8^\circ - \Delta G_2^\circ) - 0.5X + 0.5Y$
SiO_2	$Z = \kappa(\Delta G_3^\circ + \Delta G_5^\circ + \Delta G_8^\circ - \Delta G_1^\circ) - X + Y$

[a] The partial pressure, p, is expressed in atm; 1 atm = 101.3 kPa; $\kappa = -1/(4.573\,T) = -0.218\,67/T$; the numerical values of ΔG_i° are given in Table II.

The calculated results are shown in Fig. 4. Some key features of Fig. 4 will be discussed below, by focussing mainly on $Si_5C_6O_2$ or $SiC_\alpha O_\beta$ (Nicalon) at varying temperatures.

At 300–500 K, a homogeneous solid solution of $SiC_\alpha O_\beta$ can be saturated with SiC, SiO_2 or C(gr), as shown in Fig. 4a and b. Although not shown because of too narrow stability ranges [5], there exist Si_2C_3 and SiC_2 between SiC and C, and Si_2C between Si and SiC. All these minor carbides decompose and disappear above 1130 K [5]. At 1200 K $SiC_\alpha O_\beta$ can become saturated with either SiC, Si_2O_3, SiO_2 or C, as shown in Fig. 4c. These saturating species will be joined by SiO(am) at 1400 and 1500 K, Fig. 4d and e, and furthermore by Si_2O at 1600 K, Fig. 4f. Thus, the thermal decomposition of Nicalon is a complex phenomenon yielding a variety of products depending on temperature and environment, where the latter may vary from oxidizing (i.e. larger X) to reducing (i.e. smaller X) conditions, or from carburizing (i.e. higher Y) to decarburizing (i.e. lower Y) conditions [24].

The predominance diagrams not only predicate mutual relations and boundary conditions among condensed phases, but the abscissa X of oxycarbide $Si_5C_6O_2$ also indicates the CO pressure during its decomposition in a neutral environment. The solid solution $SiC_\alpha O_\beta$ coexisting with SiO_2 and C is unstable at 1400 K, because its equilibrium partial pressure of CO(g) becomes greater than 0.01 atm (or $-2 < X$), Fig. 4d (cf. the equilibrium pressure of water vapour is 0.01 atm over liquid water at 7 °C). The CO pressure over the solid solution $SiC_\alpha O_\beta$ coexisting with SiO_2 and C approaches the boiling point (i.e. $p_{CO} = 1$ atm) at 1600 K, Fig. 4f, pointing to a rapid decomposition under these conditions. Even under such a reducing condition as in coexistence with SiC, $SiC_\alpha O_\beta$ is no longer stable at 2000 K because $X > -2$, Fig. 4g. At 2400 K, the thermal decomposition of $SiC_\alpha O_\beta$ is complete under atmospheric pressure, as the vapour pressure of CO(g) over $SiC_\alpha O_\beta$ surpasses the boiling point, or $p_{CO} > 1$ atm, Fig. 4h. It is interesting to note that the decomposition of $SiC_\alpha O_\beta$ will not yield elemental silicon, because these two phases never share a common border in the predominance diagram of Fig. 4.

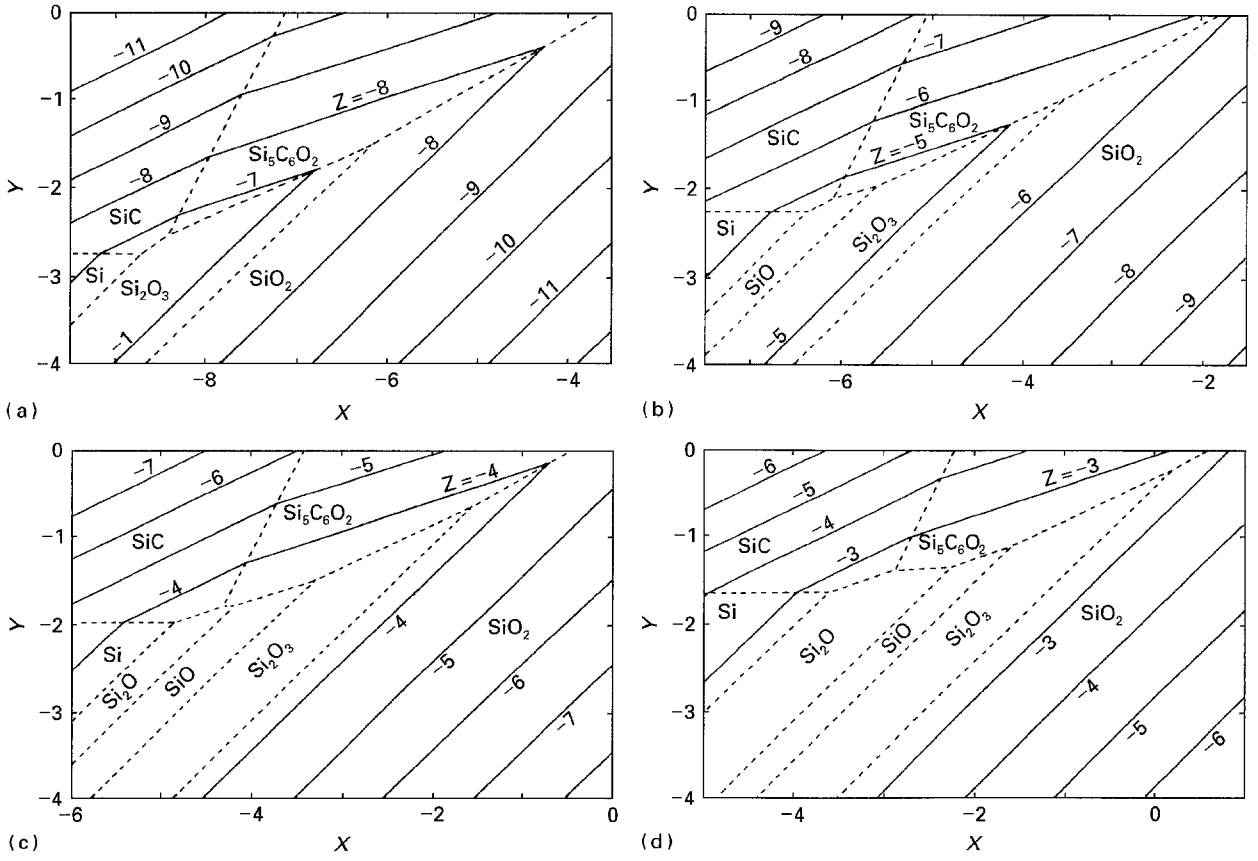

Figure 5 Partial pressure of SiO (p_{SiO}, atm) over various phases in the Si–C–O system at (a) 1200 K, (b) 1400 K, (c) 1600 K and (d) 1800 K. (---) Phase boundaries. $X \equiv \log p_{CO}$; $Y \equiv \log a_C$; $Z \equiv \log p_{SiO}$.

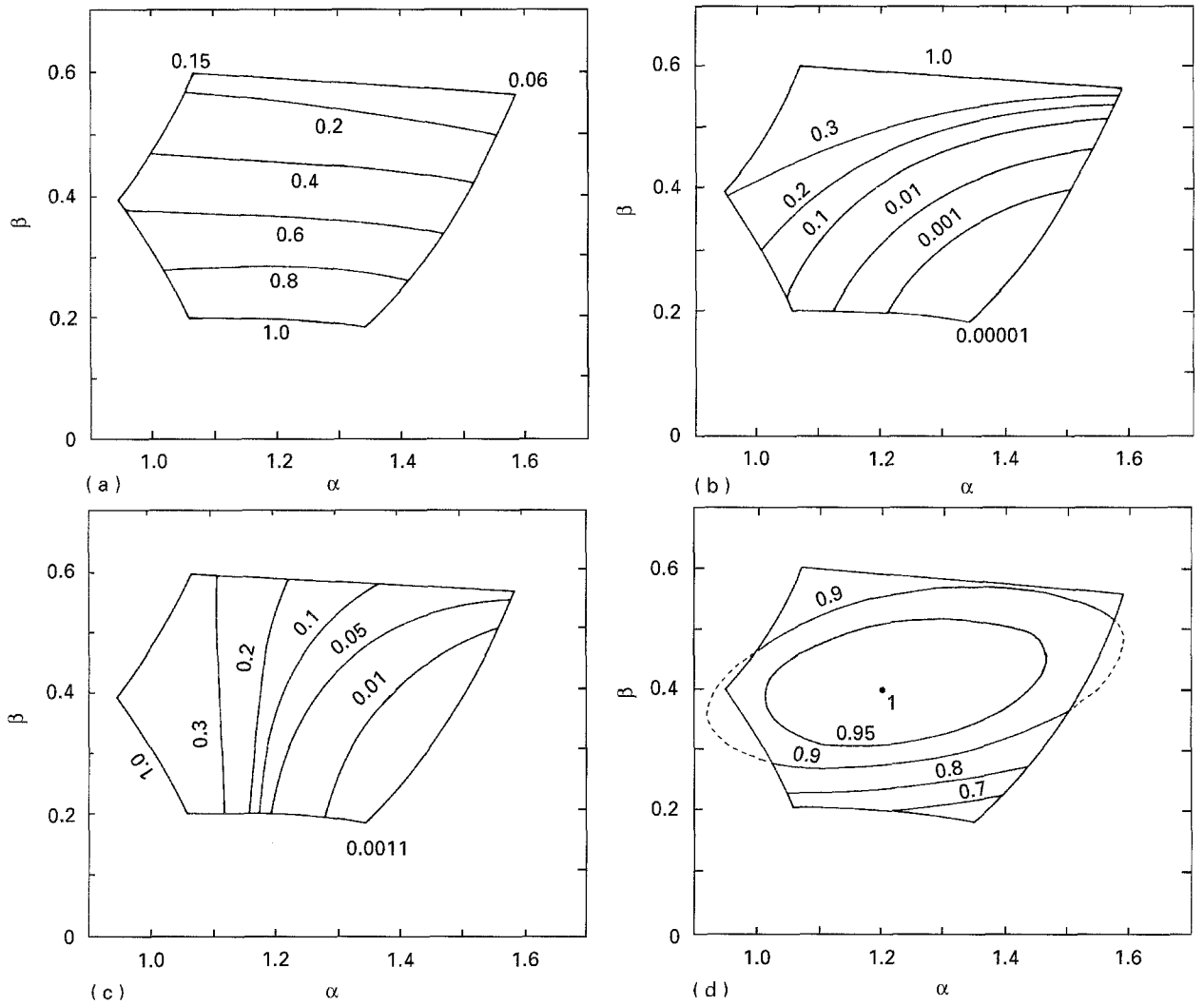

Figure 6 Variations of the Raoultian activities, a, of (a) SiC, (b) SiO_2, (c) SiO and (d) $Si_5C_6O_2$ within the homogeneous solid solution of $SiC_\alpha O_\beta$ (Nicalon) at 1500 K.

6.2. Partial pressure of SiO(g) in the Si–C–O system

In discussing the thermal instability of $SiC_\alpha O_\beta$, the equilibrium pressures of both CO(g) and SiO(g) have to be taken into account. The SiO(g) pressure over each condensed phase can be calculated [24] as a function of X and Y by combination of the Gibbs energies as summarized in Table III. Fig. 5 shows that variations of SiO(g) partial pressure over various phases at 1200–1800 K.

If an arbitrary criterion of $X \leqslant -6, Z \leqslant -6$, and $X + Z \leqslant -6$ is chosen as the condition limiting a long-term use of $SiC_\alpha O_\beta$ in an inert environment, the temperature of service has to be below about 1400 K, because virtually the entire stability zone of $SiC_\alpha O_\beta$ is situated in $-6 \leqslant X$ in Fig. 5b. Using the same criterion, Fig. 5a indicates that a long-term use of $SiC_\alpha O_\beta$, even at a lower temperature like 1200 K, has to be limited to an environment where a reducing condition prevails, because almost half of the $SiC_\alpha O_\beta$ stability zone is already situated in $-6 \leqslant X$ at 1200 K.

The oxycarbide $SiC_\alpha O_\beta$ may react with various surroundings to yield a new condensed phase such as C, SiC, Si_2O, SiO, Si_2O_3 or SiO_2 together with such gases as CO, SiO and CO_2. Depending on X and Y of the environment, the solid solution $SiC_\alpha O_\beta$ decomposes by evolving SiO(g) and CO(g) in many different ratios. For example, the equilibrium partial pressure of CO gas should be 310 times greater than that of SiO gas over the oxycarbide $SiC_\alpha O_\beta$ saturated with both SiC(s) and C(s) at 1600 K [13], because this double saturation corresponds to $X = -3.4$ and $Z = -5.9$, as shown in Fig. 5c.

The compositional (not necessarily structural) integrity of Nicalon fibres can remain permanently intact even at such a high temperature as 1800 K, as long as the coexisting gas phase contains $p_{CO} = 0.01$ atm and $p_{SiO} = 0.001$ atm, as shown in Fig. 5d. Reactions under any other different conditions can be systematically analysed and correctly predicted by use of the predominance diagram of Fig. 4 and the SiO(g) pressure diagram of Fig. 5.

6.3. Activities in $SiC_\alpha O_\beta$ at 1500 K

The Raoultian activities of SiC calculated by Equation 9 are shown in Fig. 6a. The SiC activities in the SiO_2-saturated $SiC_\alpha O_\beta$ are as low as 0.15–0.06 at 1500 K, implying that the Nicalon fibres of these compositions may show certain properties resembling silica wool. By contrast, as shown in Fig. 6b, the Raoultian

activities of SiO_2 in the SiC-saturated $SiC_\alpha O_\beta$ are below 0.08, suggesting that the Nicalon of these compositions should behave almost like SiC filaments. When $SiC_\alpha O_\beta$ is saturated with both SiC and C(gr), the SiO_2 activity becomes as low as 0.000 01, Fig. 6b, indicating that the Nicalon of this composition is void of any silica-like character and should exhibit properties akin to those of carbon fibre.

The Raoultian activities of SiO(am) are shown in Fig. 6c, and they are proportional to the decomposition pressure of SiO(g) over $SiC_\alpha O_\beta$; p_{SiO} can vary nearly 1000 times over Nicalon depending on the chemical composition. The Raoultian activity of $Si_5C_6O_2$(am) forms concentric quasi-elliptic contours around the composition $SiC_{1.2}O_{0.4}$, Fig. 6d.

All in all, Fig. 6 shows very large variations of activities within the homogeneous $SiC_\alpha O_\beta$ solid solution, suggesting that the chemical and physical properties of Nicalon fibres may vary widely with a relatively small change in the composition.

7. Conclusion

A complete set of thermodynamic properties (entropy, heat capacity, heat and Gibbs energy of formation) has been newly calculated for silicon oxycarbide $Si_5C_6O_2$ or Nicalon. The thermal stability of $Si_5C_6O_2$ depends on the oxidizing, reducing, carburizing or decarburizing potential of the surrounding environment at a given temperature. The thermal instability of $Si_5C_6O_2$ can be defined in terms of temperature and the vapour pressures of SiO(g) and CO(g) in the coexisting gas phase.

Acknowledgements

The authors thank Mr J. Gobeil and Mr J.-M. Robert, Centre de Recherches Minérales, for encouragement and continued interest, and the Quebec Government for supporting this work.

References

1. S. YAJIMA, J. HAYASHI and M. OMORI, *Chem. Lett.* **9** (1975) 931.
2. S. YAJIMA, K. OKAMURA, T. MATSUZAWA, Y. HASEGAWA and T. SHISHIDO, *Nature* **279** (1979) 706.
3. T. ISHIKAWA, H. ICHIKAWA and H. TERANISHI, in "High Temperature Materials Chemistry IV", edited by Z. A. Munir, D. Cubicciotti and H. Tagawa (The Electrochemical Society, Pennington, NJ, 1988) pp. 205–11.
4. M. NAGAMORI, J.-A. BOIVIN and A. CLAVEAU, *J. Non-cryst. Solids* **189** (1995) in press.
5. *Idem, Metall. Mater. Trans. B* **27B** (1996) to be published.
6. S. M. JOHNSON, R. D. BRITTAIN, R. H. LAMOREAUX and D. J. ROWCLIFFE, *J. Am. Ceram. Soc.* **71** (1988) C132.
7. S. M. JOHNSON, R. D. BRITTAIN and R. H. LAMOREAUX, in "High Temperature Materials Chemistry IV", edited by Z. A. Munir, D. Cubicciotti and H. Tagawa (The Electrochemical Society, Pennington, NJ, 1988) pp. 355–61.
8. E. BOUILLON, D. MOCAER, J. F. VILLENEUVE, R. PAILLER, R. NASLAIN, M. MONTHIOUX, A. OBERLIN, C. GUIMON and G. PFISTER, *J. Mater. Sci.* **26** (1991) 1517.
9. C. LAFFON, A. M. FLANK, P. LAGARDE, M. LARIDJANI, R. HAGEGE, P. OLRY, J. COTTERET, J. DIXMIER, J. L. MIQUEL, H. HOMMEL and A. P. LEGRAND, *ibid.* **24** (1989) 1503.
10. G. S. BIBBO, P. M. BENSON and C. G. PANTANO, *ibid.* **26** (1991) 5075.
11. V. BELOT, R. J. P. CORRIU, D. LECLERCQ, P. H. MUTIN and A. VIOUX, *J. Non-Cryst. Solids.* **144** (1992) 287.
12. P. GREIL, *J. Europ. Ceram. Soc.* **6** (1990) 53.
13. N. JIA, R. BODET and R. E. TRESSLER, *J. Am. Ceram. Soc.* **76** (1993) 3051.
14. J. LIPOWITZ, H. A. FREEMAN, R. T. CHEN and E. R. PRACK, *Adv. Ceram. Mater.* **2** (1987) 121.
15. T. MAH, N. L. HECHT, D. E. McCULLUM, J. R. HOENIGMAN, H. M. KIM, A. P. KATZ and H. A. LIPSITT, *J. Mater. Sci.* **19** (1984) 1191.
16. L. PORTE and A. SARTRE, *ibid.* **24** (1989) 271.
17. T. SHIMOO, H. CHEN, K. KAKIMOTO and K. OKAMURA, *J. Ceram. Soc. Jpn Int. Ed.* **101** (1993) 287.
18. Ph. SCHRECK, C. VIX-GUTERL, P. EHRBURGER and J. LAHAYE, *J. Mater. Sci.* **27** (1992) 4243.
19. A. COLSON, *C. R. Acad. Sci. Paris* **94** (1882) 1316.
20. O. KUBASCHEWSKI and C. B. ALCOCK, "Metallurgical Thermochemistry" (Pergamon Press, New York, 1979).
21. I. BARIN and O. KNACKE, "Thermochemical properties of Inorganic Substances" (Springer, New York, 1973).
22. M. NAGAMORI, K. ITO and M. TOKUDA, *Metall. Mater. Trans. B* **25B** (1994) 703.
23. T. SHIMOO and K. OKAMURA, *Funtai oyobi Funmatsu-yakin (Jpn)* **39** (1992) 447.
24. M. NAGAMORI, I. MALINSKY and A. CLAVEAU, *Metall. Trans.* **17B** (1986) 503.
25. *Idem. ibid.* **18B** (1987) 472.

Received 22 December 1994
and accepted 2 May 1995